SIMO and MIMO System Architectures and Modes for High-Resolution Ultra-Wide-Swath SAR Imaging

Gerhard Krieger, Sigurd Huber, Michelangelo Villano, Felipe Queiroz de Almeida,
Marwan Younis, Paco López-Dekker, Pau Prats, Marc Rodriguez-Cassola, Alberto Moreira
Microwaves and Radar Institute, German Aerospace Center (DLR), gerhard.krieger@dlr.de, Germany

Abstract

This paper reviews advanced SAR system architectures and modes for high-resolution ultra-wide-swath SAR imaging. The comparison includes both direct radiating array antennas and reflector-based system configurations operating in either a single-transmit multiple-receive (SIMO) or a multiple-transmit multiple-receive (MIMO) mode.

1 Introduction

Wide unambiguous swath coverage and high azimuth resolution pose contradicting requirements on the design of spaceborne SAR systems [2]. To overcome these fundamental limitations, and to enhance the capabilities and performance of future SAR systems, several new architectures, operational modes and processing techniques have been suggested that are all based on recording the scattered radar echoes with multiple sub-apertures or feed elements (cf. Figure 1). The signals from the sub-apertures/feeds are individually amplified, down-converted, and digitized. This enables an a posteriori combination of the recorded sub-aperture/feed signals to form multiple beams with time-variant adaptive shapes. The additional information about the direction of the radar echoes can then be used to (1) suppress spatially ambiguous signal returns from the ground, (2) increase the receiving antenna gain without a reduction of the imaged area, (3) suppress spatially localized interferences, and (4) gain additional information about the dynamic behaviour of the scatterers and their surroundings. By this, it becomes possible to significantly boost the performance of future spaceborne SAR systems and missions. SAR systems with multiple receiving channels are in the following denoted as single-input multiple-output (SIMO) systems. A further improvement can be achieved by using not only one, but multiple transmitters that radiate distinct waveforms [13], [25], [32]. Such systems, which have been dubbed multiple-input multiple-output (MIMO) SAR, allow not only for an enhanced suppression of ambiguities, but enable also new operational modes to satisfy hitherto incompatible user requirements regarding image resolution and coverage [13].

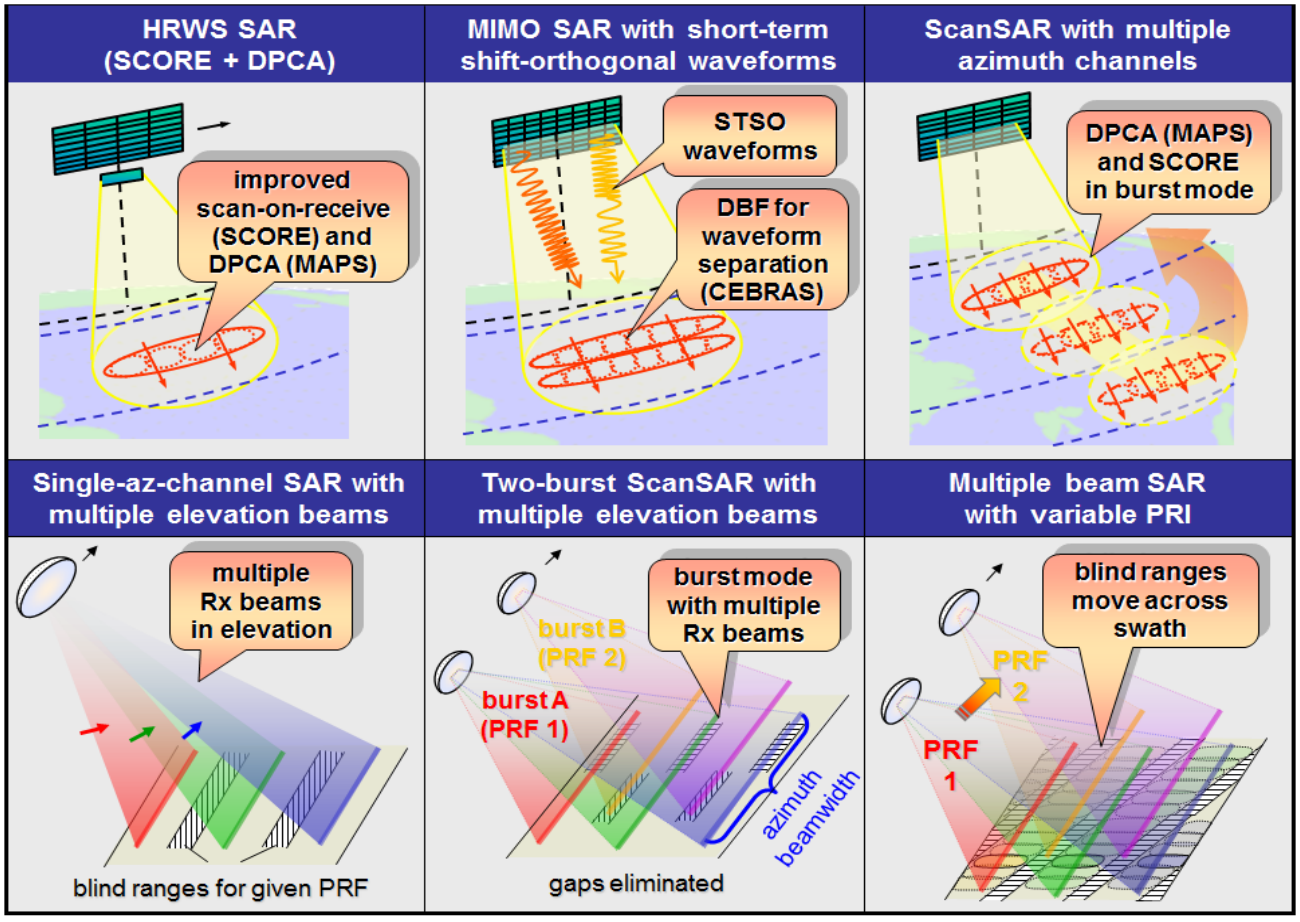

Figure 1: SAR system concepts for high-resolution wide-swath SAR imaging. From upper left to lower right: HRWS SAR with real-time digital beamforming in elevation and multiple Rx channels in azimuth [7], MIMO SAR with multiple azimuth channels [13], [25], [32], ScanSAR with multiple azimuth channels [15], [20], [21], reflector SAR with multiple elevation beams [15], [19], [22], two-burst ScanSAR with multiple elevation beams [15], and SAR with continuous PRI variation [16], [15], [27], [30].

ISBN 978-3-8007-4228-8 / ISSN 2197-4403

2 System Architectures and Modes

Regarding the architecture of SIMO and MIMO systems, two basic configurations can be distinguished. The first employs multiple azimuth antennas and/or beams in the along-track direction [4], while the second employs multiple beams and/or Rx channels in the elevation direction [3]. In principle, it is also possible to combine both techniques for the implementation of an advanced high-resolution wide-swath SAR imaging system [6], [7].

2.1 Stripmap SAR with Multiple Azimuth Channels

Stripmap SAR systems with multiple azimuth channels are well suited to obtain a fine azimuth resolution over a moderate swath width (e.g. 1 m @ 100 km). For this, the scene is illuminated by a wide transmit beam and the radar echoes are recorded by a long receiving antenna that is divided in the along-track direction into multiple short sub-apertures, each connected to an individual receiving channel. Every sub-aperture element will then receive signals from a wide Doppler spectrum, as required for obtaining a high azimuth resolution. Hence, a high pulse repetition frequency (PRF) would be needed to avoid azimuth ambiguities. Such a high PRF can, however, be avoided by combining the signals from the multiple displaced azimuth sub-apertures. For this, a dedicated reconstruction algorithm has been developed that performs a frequency dependent linear superposition of the signals from the N ambiguous azimuth channels, each sampled with PRF, to obtain a single unambiguous azimuth signal, sampled with $N \cdot PRF$, [11], [17]. As illustrated in Figure 2, this multi-aperture reconstruction can also be regarded as a frequency-dependent null steering that suppresses, for each Doppler frequency, the corresponding azimuth ambiguities. As the minimum angular separation $\Delta\varphi$ between the centre of a beam with maximum gain and its corresponding nulls is given by $\Delta\varphi \geq \lambda/l_{ant}$, it is only possible to resolve mutually ambiguous Doppler frequencies that exceed $\Delta f_{Dop} \geq 2v_{sat}/\lambda \cdot \Delta\varphi$ without compromising the antenna gain in the direction of the desired Doppler frequency. Here, λ is the wavelength, v_{sat} is the satellite velocity and l_{ant} is the total antenna length. To ensure a good ambiguity suppression, the PRF has therefore to be chosen such that $PRF \geq 2v_{sat}/l_{ant}$.

A similar improvement of the azimuth resolution can be obtained by a SIMO SAR that employs a reflector antenna in combination with multiple azimuth feed elements [14], [19], [22]. Here, each feed is associated with a narrow beam that records a small portion of the total Doppler spectrum.

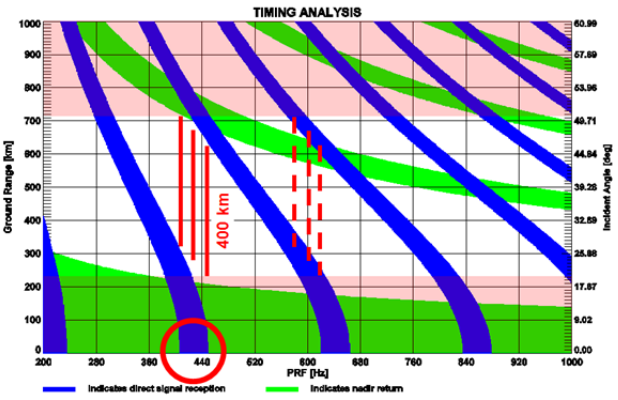

Figure 3: Timing for a satellite height of $h_{sat} = 700$ km and a duty cycle of $\Delta_{duty} = 10\%$.

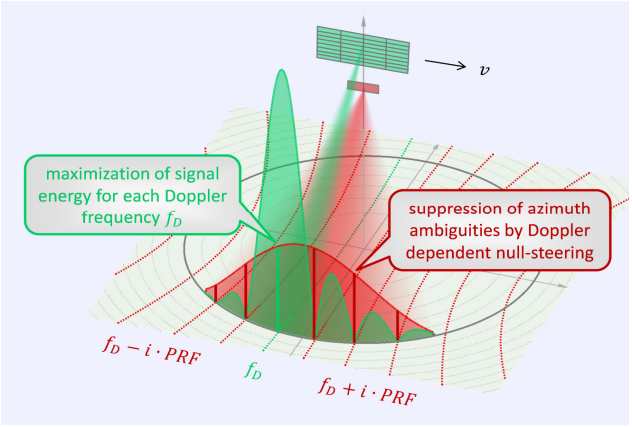

Figure 2: The azimuth ambiguity suppression in the range-Doppler domain can be regarded as digital beamforming on receive where for each considered Doppler frequency f_D a narrow beam with high gain is steered towards the direction of f_D and, at the same time, a set of nulls are steered towards the corresponding azimuth ambiguities at $f_D + i \cdot PRF$. By repeating the beamforming for each desired Doppler frequency f_D a broad azimuth spectrum can be recovered without ambiguities from the recorded multi-channel SAR data [11], [17], [22], [28], [29], [38].

By combining the signals from the multiple azimuth feeds, a wide Doppler spectrum can be recovered. This can, e.g., be achieved by employing, for each Doppler frequency, a linear constraint minimum variance (LCMV) beamformer to suppress the corresponding azimuth ambiguities [22]. As this ambiguity suppression performs essentially a null-steering, it is equivalent to the aforementioned multi-aperture reconstruction algorithm, and can, if necessary, be easily extended to other beamformers [28], [29], [38].

A drawback of the stripmap configuration with multiple azimuth channels is the very long antenna that is required to map a wide swath. As an example, we consider a swath width of 400 km which allows for a weekly global revisit. Assuming a 700 km orbit and an incident angle above 25°, the maximum PRF is in the order of 425 Hz (cf. Figure 3). The required antenna length can be computed as $l_{ant} \geq 2v_{sat}/PRF$, which yields for $PRF = 425$ Hz and $v_{sat} = 7.5$ km/s a minimum antenna length of $l_{ant} \gtrsim 35$ m. To achieve an azimuth resolution of, e.g., $\delta_{az} = 3$ m, the required number of azimuth channels would be $N_{az} \geq 6$. It may be challenging and costly to deploy a planar array antenna with a length of $l_{ant} \gtrsim 35$ m in space.

2.2 MIMO SAR with Multiple Azimuth Channels

A possible technique to reduce the antenna length is the operation in a MIMO-SAR mode where the leading and trailing edges of the antenna are used to simultaneously transmit two orthogonal pulses [13], [25], [32]. As illustrated in Figure 5, this allows for the acquisition of additional phase centres for each transmitted pulse pair. As the resulting phase centres cover, if compared to the approach of Section 2.1, twice the azimuth interval this enables, for the considered swath width of 400 km, a notable reduction of the antenna length from $l_{ant} \gtrsim 35$ m to $l_{ant} \approx 20$ m.[1] Such a value is

[1] A comparable improvement can be achieved by multi-dimensional waveform encoding in azimuth where the full antenna length is used to illuminate a wide Doppler spectrum via a set of narrow azimuth beams that transmit, e.g., a sequence of sub-pulses [13], [23], [31]. This implementation is also well suited for a reflector-based system with multiple azimuth feeds [14].

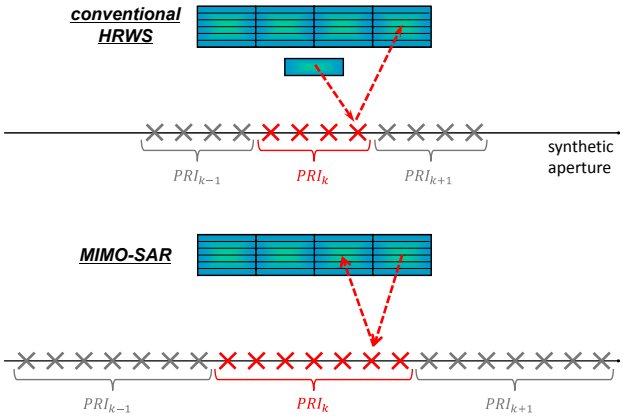

Figure 5: Additional phase centres provided by a MIMO SAR for high-resolution wide-swath SAR imaging. (Top) azimuth phase centres for a SIMO SAR where multiple displaced sub-apertures record the radar echoes from a single transmitter (cf. [4]). (Bottom) MIMO SAR where the left and right sub-apertures transmit short-term shift-orthogonal (STSO) waveforms that can be separated by digital beamforming on receive in elevation. The MIMO SAR provides, for each transmitted pulse, more phase centres and covers therefore a wider span of the synthetic aperture. Hence, a lower PRF can be used which allows for the mapping of a wider swath.

much closer to the 15 m antenna length that has already been deployed in orbit for Radarsat-2, but it is still considered a challenge and cost driver. Moreover, a sufficient antenna height h_{ant} has to be provided to separate the short-term shift-orthogonal (STSO) waveforms by digital beamforming in elevation [13], [23], [25], [31], [32]. Assuming that the two waveforms keep their orthogonality for an interval of $\Delta\tau_{STSO} = 200$ µs (i.e. 8.5% of the pulse repetition interval for a PRF of 425 Hz) as well as an orbit height of $h_{sat} = 700$ km and a maximum incident angle of $\theta_{i,max} = 50°$, the required antenna height is approximately 10 m in L band, 2.5 m in C band, and 1.4 m in X band (cf. Figure 4). The antenna height could in principle be reduced by increasing $\Delta\tau_{STSO}$, but this would be in conflict with the required swath width and the timing diagram.

To summarize, the proposed MIMO SAR may be an interesting candidate for an X- or C-band system if a very high resolution in the meter or even decimetre range is required over a swath width in the order of 200-300 km. Such a system allows for a transmit PRF above 600 Hz, and therefore a reduction of the antenna length to 12-15 m. The required antenna height depends on the STSO interval and therefore on both the timing diagram and the swath width. As a first approximation, antenna heights in the order of 1.5 m and 3 m should be sufficient in X and C band, respectively, to map a 250 km wide swath if an advanced range ambiguity suppression technique like CEBRAS is employed to separate the STSO waveforms [35].

2.3 ScanSAR with Multiple Azimuth Channels

Another possibility for high-resolution ultra-wide-swath imaging is the multi-channel ScanSAR (or TOPS) mode that is illustrated in Figure 1 on the upper right.[2] This mode employs multiple azimuth channels to achieve a high resolution in the along-track direction and, in addition, a ScanSAR operation to map a wide swath with a moderate antenna length [15], [20], [21]. Assuming an antenna length of 12 m, the minimum PRF is in the order of 1.25 kHz. A timing analysis reveals that at least 4 bursts would be required to cover a 400 km swath without nadir returns. The azimuth resolution of a conventional single-channel ScanSAR would then be $\delta_{az} > (N_{burst} + 1) \cdot l_{ant}/2 = 30$ m. To achieve an azimuth resolution of, e.g., $\delta_{az} = 5$ m one may employ multiple azimuth channels, where the minimum number of channels is $N_{az} > l_{ant} \cdot (N_{burst} + 1)/(2\delta_{az})$ [15]. Hence, at least 7 channels will be required, and a more detailed ambiguity analysis using the exact shape of the Tx pattern may result in even a higher number of azimuth channels. Further challenges arise also for the multi-aperture processing due to the varying target Doppler spectra together with the required variation of the PRF values that may, at least for some bursts, result in a significant deviation from the optimum uniform sampling [20].

The previous analysis revealed that the mapping of a wide swath with a reasonably short antenna may require a rather large number of bursts. In consequence, significant variations of the Doppler centroids will be observed for different along-track positions within the SAR image. The corresponding squint angles cover an interval that may be approximated as $\Delta\psi \approx (N_{burst} + 1) \cdot \lambda/2\delta_{az}$. Assuming, e.g., an L-band SAR with 5 m azimuth resolution and 4 bursts, this yields a squint angle variation of $\Delta\psi \approx 6.8°$. The high squint angles and their variations during the SAR data acquisition may have several detrimental implications for SAR imaging and SAR interferometry. Examples are a rather large range cell migration, significant variations in the line-of-sight angle for deformation and target motion measurements [26], as well as discontinuities among the burst transitions due to atmospheric propagation effects. Especially for low frequency SAR systems, the latter may become an annoying error source, as it has, e.g., been shown in [34] that already rather small variations in the look angle may be associated with significant ionospheric phase disturbances. As such effects have already been observed at the burst transitions of TOPS acquisitions with TerraSAR-X and Sentinel-1A [39], and as these effects increase with both the wavelength and the squint angle difference, they may become challenging for future low frequency high-resolution ultra-wide-swath SAR systems that intend to use the multi-channel ScanSAR mode with its inherently large squint angle variations.

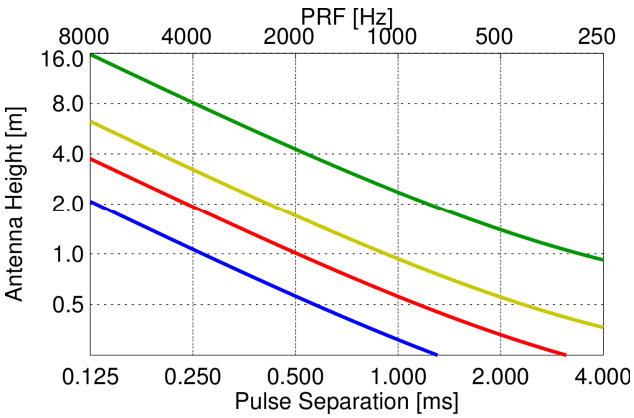

Figure 4: Minimum antenna height for L (green), S (yellow), C (red), and X (blue) band. The maximum incident angle is $\theta_{i,max} = 50°$, and the satellite height is $h_{sat} = 700$ km.

[2] Such a high-resolution ScanSAR mode can also be implemented with a reflector-based system that employs multiple azimuth feeds which are connected to separate receiving channels.

2.4 SAR Systems with Multiple Elevation Beams

The system architectures discussed in Sections 2.1 to 2.3 used essentially multiple azimuth channels to resolve the contradicting requirements between azimuth resolution and swath width. In addition, it was implicitly assumed that these systems use also the scan-on-receive (SCORE) or Sweep-SAR technique which employs an enlarged elevation aperture in combination with real-time beamforming on receive to obtain a high antenna gain towards the expected direction of the arriving radar echoes [1], [5], [7], [9], [18]. As the scan-on-receive technique requires anyway multiple elevation channels, it may be worth to consider also SAR systems that form from the received sub-aperture or feed signals not only one but multiple elevation beams at the same time [3]. An example for such a system is illustrated on the lower left of Figure 1. The system illuminates a wide swath with a high PRF as required to obtain a fine azimuth resolution. In consequence, the radar echoes from multiple transmitted pulses will arrive simultaneously at the radar. In a conventional SAR, these echoes would be regarded as annoying range ambiguities, but by taking advantage of the high receiving aperture and the multiple elevation channels one may form not only one but multiple narrow elevation beams, each following the radar echo of a different transmitted pulse. By this, it becomes possible to map multiple swaths at the same time. The individual swaths are, however, separated by blind ranges, as a spaceborne radar can typically not transmit and receive at the same time. Several options to avoid such gaps in the SAR image will be discussed in the following sections. If compared to systems with multiple azimuth apertures, systems with multiple elevation beams may have the following benefits:

- Only a single azimuth channel is required to map a wide image swath with high azimuth resolution. This avoids the duplication of hardware for multiple azimuth channels and can therefore significantly reduce the system complexity, power demands, mass and costs.
- A wide image swath can be mapped using neither a long antenna nor the ScanSAR mode with its possible challenges due to the high squint angle variations.
- SAR systems with multiple elevation beams may lead in many cases to a compact antenna architecture where the antenna height and length are well balanced. This supports the employment of alternative antenna types by replacing, for example, a long direct radiating array with a circular reflector illuminated by a digital feed array.
- The use of a single azimuth channel supports the employment of advanced on-board data compression techniques [36], while a system with multiple azimuth channels may first need a reconstruction of the unambiguous SAR signal from all azimuth channels.

A main challenge for the implementation of a multiple swath SAR system is the suppression of range ambiguities and nadir echoes. While range ambiguity suppression in a conventional SAR benefits from the combined two-way transmit and receive antenna pattern, it has now to be performed by relying solely on digital beamforming on receive. An interesting technique to support this objective is the hybrid on-board/on-ground beamforming approach CEBRAS, which allows for an efficient suppression of range ambiguities also in case of non-ideal antenna patterns, pointing-errors and topographic variations [35].

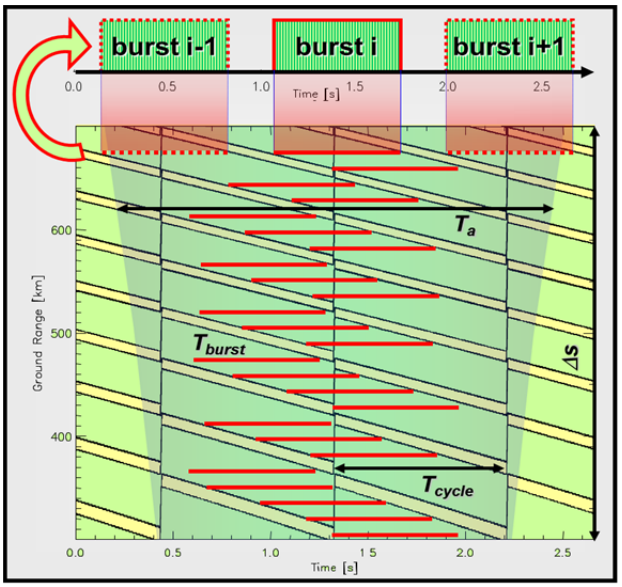

wavelength	λ	0.056 m	minimum PRF	PRF_{min}	5000 Hz
satellite height	h_{sat}	750 km	maximum PRF	PRF_{max}	5145 Hz
incident angles	θ_{inc}	24° - 48°	cycle time	T_{cycle}	0.89 s
swath width	Δs	**400 km**	azimuth beam time min	$T_{a,min}$	1.8 s
azimuth resolution near	Δaz_{near}	**4.5 m**	azimuth beam time max	$T_{a,max}$	2.3 s
azimuth resolution far	Δaz_{far}	**5.8 m**	burst length	T_{burst}	> 0.65 s
antenna length	l_{ant}	3 m	Tx duty cycle	Δ_{duty}	10 %
antenna height	h_{ant}	> 2.5 m	elevation beams	N_{el}	9

Figure 6: Two-burst ScanSAR with multiple elevation beams and slow PRI variation. Top: Illustration of burst positions for different slant ranges. The dark green area shows the extension of the 3-dB antenna footprint in azimuth. Bottom: Exemplary parameters for the corresponding C-band SAR system.

A further challenge may arise for the suppression of nadir echoes. Here, a reflector-based system could have the advantage to reduce the illumination in the nadir direction, thereby avoiding possible saturation effects in the relevant receiver channels that might arise in case of very strong nadir returns. The strength of the nadir signal can further be reduced by a careful design of the Tx antenna pattern and, if necessary, an appropriate adaptation of the scan-on-receive technique by steering a fixed null towards the nadir direction (either on-board in real-time or a posteriori with CEBRAS via the acquisition of some extra radar echoes via a fixed nadir beam). An additional improvement can be achieved by varying the waveforms among the transmitted pulses which allows for a spread of the nadir energy in the range-focused echoes. A further option is a variation of the pulse repetition interval (PRI) which will be discussed in more detail later in this chapter.

2.5 Two-Burst ScanSAR with Multiple Elevation Beams

In Section 2.3 we discussed a high-resolution ScanSAR mode with multiple azimuth channels. A possible drawback of this mode may be the rather high variation of the squint angles that are, especially for low frequencies, required to map with a compact antenna an ultra-wide swath with high azimuth resolution. The squint angle variation can, however, be mitigated by reducing the number of bursts. Such a reduction becomes possible by using not only one but multiple elevation beams at the same time. In this case, two bursts with slightly different PRFs are, in principle, sufficient to map an ultra-wide swath if it is possible to suppress nadir echoes by digital beamforming on receive (cf. illustration in the lower middle of Figure 1).

ISBN 978-3-8007-4228-8 / ISSN 2197-4403

The use of multiple elevation beams favours the use of more compact antennas with less azimuth channels. As an example, consider a system with a single azimuth channel. To achieve an azimuth resolution of, e.g., $\delta_{az} = 5$ m with two bursts, the antenna length should be in the order of $l_{ant} \approx 3$ m. To avoid azimuth ambiguities, the PRF has then to be above 5 kHz. Assuming again an orbit height of $h_{sat} = 700$ km and a maximum incident angle of $\theta_{i,max} = 50°$, the minimum antenna height to separate the pulses from the different swaths is in the order of 10 m in L band, 2.5 m in C band, and 1.4 m in X band (cf. Figure 4).

The required antenna height can, of course, be reduced on the cost of an increased antenna length by employing not only one but multiple azimuth phase centres. For example, two azimuth phase centres may allow for a more compact L-band antenna configuration by reducing in the previous example the minimum antenna height from 10 m to 5 m while increasing the antenna length from 3 m to 6 m. Such a system could also be well implemented by a reflector-based configuration that employs a digital feed with multiple elevation and azimuth channels [22].

2.6 Two-Burst ScanSAR with Slow PRI Variation

An inherent peculiarity of the multiple-beam ScanSAR mode is the constant burst length for all sub-swaths. As a result, the azimuth resolution will vary with range. The performance of the two-burst multiple-elevation-beam ScanSAR mode can be improved by using additional PRF values or even a slow continuous variation of the PRF during the target exposure time as illustrated in the lower right of Figure 1. An example of such a system is sketched in Figure 6, where we consider a periodic linear PRF increase from 5000 Hz to 5145 Hz which shifts the blind ranges smoothly across the swath. For each range, one obtains then a contiguous burst which is longer than that for the twin PRF case. The SAR focusing of the individual bursts requires, however, a (simple and straight-forward) interpolation of the azimuth raw data to a uniform sampling interval.

2.7 Staggered SAR

Sections 2.3 to 2.6 used burst modes to map an ultra-wide swath with a compact antenna. An alternative is a stripmap mode with multiple elevation beams. Here, the emergence of blind ranges can be avoided by a fast variation of the PRI as originally suggested in [16], [15] and elaborated in detail in [27], [30]. This staggered SAR mode has also been selected as baseline for Tandem-L, which uses a deployable reflector with a diameter of 15 m in combination with a digital feed array [33], [42]. Figure 7 shows, as an example, the range and azimuth ambiguities for an L-band staggered SAR that covers a 400 km wide swath with an azimuth resolution of 5 m. The system has an excellent performance where the ambiguity-to-signal ratio is always below -25 dB. The NESZ varies between -32 dB and -25 dB in near and far range, respectively, assuming a peak transmit power of 5.3 kW and a pulse duty cycle of 6%, which corresponds to an average radiated power of only 320 W. A challenge of staggered SAR is the required azimuth oversampling which implies a high mean PRF and therefore a high data rate. To overcome this problem, a new on-board data compression technique has been proposed which allows for an efficient data reduction that even excels that of conventional SAR systems in terms of the required bits per image pixel [36].

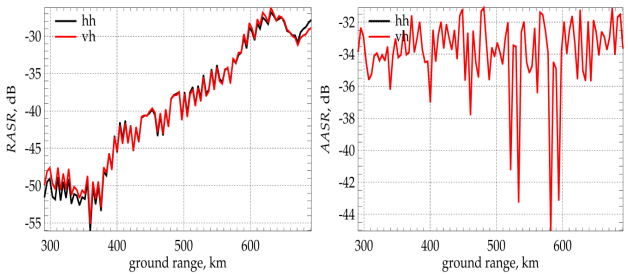

Figure 7: Range (left) and azimuth (right) ambiguities for an L-band staggered SAR system employing a 15 m reflector with a 7.15 m x 0.86 m offset feed to cover a 400 km wide swath with an azimuth resolution of 5 m. The feed has 50 digital elevation channels, each combining signals from 6 azimuth patches.

2.8 Staggered SAR with Multiple Azimuth Channels

The staggered SAR mode is a promising solution to map an ultra-wide swath with an azimuth resolution in the order of $\delta_{az} = 5$ m which requires an effective aperture length in the order of $l_{ant} \approx 10$ m. A very high azimuth resolution in the order of $\delta_{az} = 1$ m or below would, however, require a rather short antenna in combination with very short pulse repetition intervals of less than 0.1 ms to avoid azimuth ambiguities. Hence a very high antenna would be required to suppress range ambiguities and the associated narrow elevation beams may affect the SAR performance due to topographic variations, attitude errors, etc. Such problems can be avoided by adding again additional azimuth apertures or feed elements in the along-track direction. A new processing technique is, however, required to combine the staggered SAR mode with an antenna architecture that comprises multiple azimuth channels. Such a technique has been developed in [43] for a reflector-based system by taking advantage of the phase centre shift technique from [37]. A similar approach can also be applied for a planar staggered SAR system with multiple azimuth channels. Such a system is well suited for future missions that shall map ultra-wide swaths with very high azimuth resolution.

3 Discussion

This paper discussed several SAR system architectures and modes for high-resolution ultra-wide-swath SAR imaging. Systems with multiple azimuth apertures need either a pretty long antenna or an operation in a multichannel ScanSAR/TOPS mode to obtain a wide swath. Multi-channel ScanSAR may face challenges for low frequency SAR systems, as it implies a rather high variation of the squint angles. An alternative are SAR systems with multiple elevation beams. Here, a systematic variation of the pulse repetition interval in either a two-burst ScanSAR or a staggered SAR mode is a promising technique for ultra-wide swath SAR imaging. Finally, the combination of staggered SAR with multiple azimuth channels poses great potential for the imaging of ultra-wide swaths with very high azimuth resolutions and without blind ranges.

A further option for high-resolution wide-swath imaging is a distributed SAR [8]. Here, a bistatic SAR allows for the simultaneous pulse transmission and reception thereby avoiding the blind-range problem in a multiple elevation beam SAR [10]. Additional opportunities arise in reconfigurable fully-active SAR systems which may serve several purposes like along-track and cross-track interferometry and tomography in concert with ambiguity suppression for high-resolution wide-swath SAR imaging [12], [24], [40],

[41]. An appropriately designed MIMO-SAR system with N fully-active satellites may, for example, achieve a performance gain of N^2 if compared to a gain of N for a constellation of N independently operated satellites. This gain is due to the fact that each satellite collects the transmitted signal energy from all other satellites. Moreover, if compared to a monostatic MIMO SAR, the separation of the multiple STSO Tx signals is alleviated as the whole PRI interval can now be exploited for signal transmission. This supports the use of smaller satellites.

References

[1] J.H. Blythe, "Radar Systems," US Patent 4253098, 1981.

[2] J. Curlander, R. McDonough, "Synthetic Aperture Radar: Systems and Signal Processing," Jon Wiley & Sons, 1991.

[3] H.D. Griffiths, P. Mancini, "Ambiguity suppression in SARs using adaptive array techniques," in Proc. IGARSS, 1991.

[4] A. Currie, M.A. Brown, "Wide-swath SAR," IEE Proc. F - Radar and Signal Processing, vol. 139, pp. 122-135, 1992.

[5] J.T. Kare, "Moving receive beam method and apparatus for synthetic aperture radar," US 6175326 B1, June 29, 1998.

[6] G.D. Callaghan, I.D. Longstaff, "Wide-swath space-borne SAR using a quad-element array," IEE Proceedings for Radar, Sonar and Navigation, Vol. 146, pp. 159-165, 1999.

[7] M. Suess, B. Grafmueller, R. Zahn, "A novel high resolution, wide swath SAR system", Proc. IGARSS, pp. 1013-15, 2001.

[8] N. Goodman, S. Lin, D. Rajakrishna, J. Stiles, "Processing of multiple-receiver spaceborne arrays for wide-area SAR," IEEE Trans. Geosci. Remote Sens., Vol. 40, pp. 841-852, 2002.

[9] M. Younis, C. Fischer, W. Wiesbeck, "Digital beamforming in SAR systems," IEEE Trans. Geosci. Remote Sens., Vol. 41, pp. 1735-39, 2003.

[10] G. Krieger, A. Moreira, "Potential of digital beamforming in bi- and multistatic SAR," Proc. IGARSS, pp. 527-529, 2003.

[11] G. Krieger, N. Gebert, A. Moreira, "Unambiguous SAR signal reconstruction from non-uniform displaced phase centre sampling," IEEE Geosci. Remote Sens. Letters, Vol. 1, pp. 260-264, 2004.

[12] G. Krieger, A. Moreira, "Spaceborne bi- and multistatic SAR: potential and challenges," IEE Proceedings - Radar, Sonar and Navigation, Vol. 153, pp. 184-198, 2006.

[13] G. Krieger, N. Gebert, A. Moreira, "Multidimensional waveform encoding: A new digital beamforming technique for synthetic aperture radar remote sensing," IEEE Trans. Geosci. Remote Sens., Vol. 46, No. 1, pp. 31-46, 2008.

[14] G. Krieger, N. Gebert, M. Younis, A. Moreira, "Advanced synthetic aperture radar based on digital beamforming and waveform diversity," Proc. IEEE RadarCon, Rom, Italy, 2008.

[15] G. Krieger, N. Gebert, M. Younis, F. Bordoni, A. Patyuchenko, A. Moreira, "Advanced Concepts for Ultra-Wide-Swath SAR Imaging," in Proc. EUSAR, pp. 31-34, June 2008.

[16] B. Grafmueller, C. Schaefer, "High resolution synthetic aperture radar device and antenna for one such radar," US 2009/0079621 A1.

[17] N. Gebert, G. Krieger, A. Moreira. "Digital beamforming on receive: Techniques and optimization strategies for high resolution wide-swath SAR imaging," IEEE Trans. Aerospace Electronic Systems, Vol. 45, pp. 564-592, 2009.

[18] A. Freeman, G. Krieger, P. Rosen, M. Younis, W. Johnson, S. Huber, R. Jordan, A. Moreira, "SweepSAR: beam-forming on receive using a reflector-phased array feed combination for spaceborne SAR," in Proc. RadarCon, Pasadena, USA, 2009.

[19] M. Younis, S. Huber, A. Patyuchenko, F. Bordoni, G. Krieger, "Performance comparison of reflector- and planar-antenna based digital beam-forming SAR," International Journal of Antennas and Propagation, 2009.

[20] N. Gebert, G. Krieger, A. Moreira. "Multichannel azimuth processing in ScanSAR and TOPS mode operation," IEEE Trans. Geosci. Remote Sens., Vol. 48, pp. 2994-3008, 2010.

[21] M. Ludwig, C. Buck, S. D'Addio, R. Torres, F. Rostan, C. Schaefer, R. Croci, "Earth observation instruments with e-scan antennas state-of-the-art and outlook," in Proc. IEEE MTT-S International Microwave Symposium Digest, May 23-28, 2010.

[22] S. Huber, M. Younis, A. Patyuchenko, G. Krieger, A. Moreira, "Spaceborne Reflector SAR Systems with Digital Beamforming," IEEE Trans.Aerospace Electronic Systems, Vol. 48, pp. 3473-93, 2012.

[23] F. Feng, S. Li, W. Yu, P. Huang, W. Xu, "Echo separation in multidimensional waveform encoding SAR remote sensing using an advanced null-steering beamformer," IEEE Trans. Geosci. Remote Sens., Vol. 50, pp. 4157-72, 2012.

[24] M. Rodriguez-Cassola et al., "Cross-platform spaceborne SAR imaging: demonstration using TanDEM-X," IGARSS 2013.

[25] G. Krieger, "MIMO-SAR: Opportunities and pitfalls," IEEE Trans. Geosci. Remote Sens., Vol. 52, pp. 2628-2645, 2014.

[26] F. De Zan, P. Prats-Iraola, R. Scheiber, A. Rucci, "Interferometry with TOPS: coregistration and azimuth shifts", Proc. EUSAR, pp. 949-952, 3-5 June 2014.

[27] M. Villano, G. Krieger, A. Moreira, "Staggered SAR: High-resolution wide-swath imaging by continuous PRI variation," IEEE Trans. Geosci. Remote Sens., Vol. 52, pp. 4462-79, 2014.

[28] D. Cerutti-Maori, I. Sikaneta, J. Klare, C. Gierull, "MIMO SAR processing for multichannel high-resolution wide-swath radars," IEEE Trans. Geosci. Remote Sens., Vol. 52, pp. 5034-55, 2014.

[29] I. Sikaneta, C. Gierull, D. Cerutti-Maori, "Optimum signal processing for multichannel SAR: With application to high-resolution wide-swath imaging," IEEE Trans. Geosci. Remote Sens., Vol. 52, pp. 6095-6109, 2014.

[30] M. Villano, G. Krieger, A. Moreira, "A Novel Processing Strategy for Staggered SAR," IEEE Geosci. Remote Sens. Letters, Vol. 11, pp. 1891-95, 2014.

[31] F. He, X. Ma, Z. Dong, D. Liang, "Digital beamforming on receive in elevation for multidimensional waveform encoding SAR sensing," IEEE Geosci. Remote Sens. Letters, Vol. 11, pp. 2173-77, 2014.

[32] J.H. Kim, M. Younis, A. Moreira, W. Wiesbeck, "Spaceborne MIMO synthetic aperture radar for multimodal operation," IEEE Trans. Geosci. Remote Sens., Vol. 53, pp. 2453-66, 2015.

[33] A. Moreira et al., "Tandem-L: A highly innovative bistatic SAR mission for global observation of dynamic processes on the Earth's surface," IEEE Geosci. Mag., Vol. 3, pp. 8-23, 2015.

[34] G. Krieger, F. De Zan, P. Lopez Dekker, J.S. Kim, M. Rodriguez-Cassola, A. Moreira, "Impact of TEC gradients and higher-order ionospheric disturbances on spaceborne single-pass SAR interferometry," in Proc. IGARSS, July 2015.

[35] G. Krieger, S. Huber, M. Villano, M. Younis, T. Rommel, P. Lopez Dekker, F. Queiroz de Almeida, A. Moreira, "CEBRAS: Cross elevation beam range ambiguity suppression for high-resolution wide-swath and MIMO SAR imaging," in Proc. IGARSS, July 2015.

[36] M. Villano, G. Krieger, A. Moreira, "Data volume reduction in high-resolution wide-swath SAR systems," Proc. APSAR, September 2015.

[37] S. Bertl, P. Lopez Dekker, M. Younis, G. Krieger, "Along-track SAR interferometry using a single reflector antenna," IET Radar, Sonar & Navigation, Vol. 9, pp. 942-947, 2015.

[38] B. Liu, Y. He, "Improved DBF algorithm for multichannel high-resolution wide-swath SAR," IEEE Trans.Geosci. Remote Sens., Vol. 54, pp. 1209-25, June 2016.

[39] P. Prats et al., "Demonstration of the applicability of 2-look burst modes in non-stationary scenarios with TerraSAR-X," Proc. EUSAR, June 2016.

[40] T. Kraus et al. "Multistatic SAR imaging: first results of a four phase center experiment with TerraSAR-X and TanDEM-X," Proc. EUSAR, June 2016.

[41] J. Mittermayer et al., "Small satellite dispersed SAR - an exemplary configuration," Proc. EUSAR, June 2016.

[42] S. Huber et al., "Tandem-L: design concepts for a next-generation spaceborne SAR system," Proc. EUSAR, June 2016.

[43] F. Queiroz de Almeida et al, "Multichannel staggered SAR azimuth sample regularization", Proc. EUSAR, June 2016.